Cell Reports
Methods

Article

SOX17/ETV2 improves the direct reprogramming of adult fibroblasts to endothelial cells

Graphical abstract

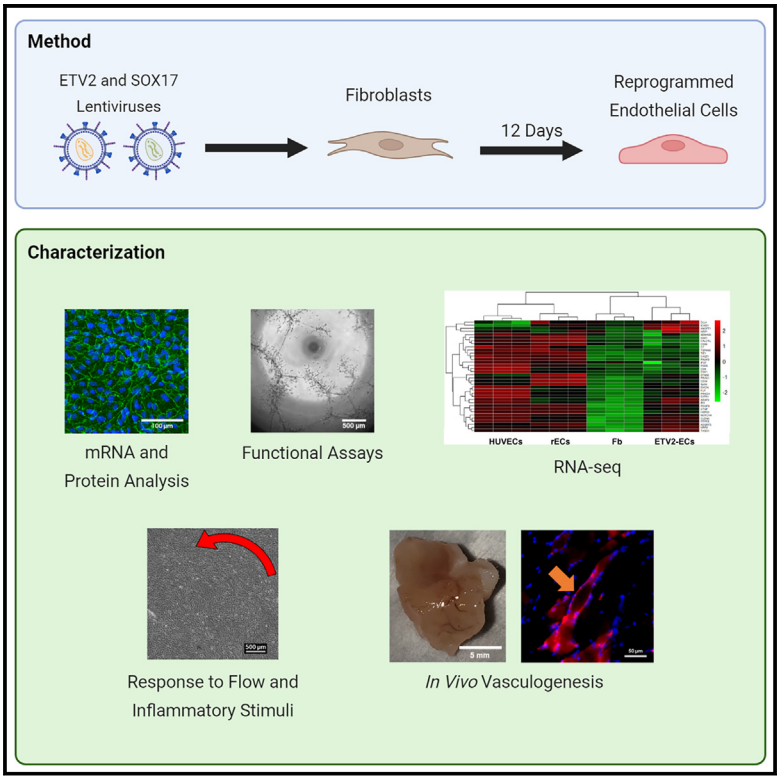

Highlights

- An improved method for generating vascular endothelial cells from fibroblasts (rECs)
- Combining SOX17 and ETV2 expression enhances reprogramming efficiency
- rECs show increased enrichment for endothelial gene expression
- rECs form large blood vessels connecting to the host and express eNOS *in vivo*

Authors

Alexander Grath, Guohao Dai

Correspondence

g.dai@northeastern.edu

In brief

Grath et al. develop an improved method of directly reprogramming adult human dermal fibroblasts into vascular endothelial cells using SOX17 and ETV2. This approach enhances reprogramming efficiency and endothelial cell characteristics, such as eNOS expression.

Grath & Dai, 2024, Cell Reports Methods *4*, 100732
March 25, 2024
https://doi.org/10.1016/j.crmeth.2024.100732

CellPress

Cell Reports Methods

CellPress
OPEN ACCESS

Article

SOX17/ETV2 improves the direct reprogramming of adult fibroblasts to endothelial cells

Alexander Grath[1] and Guohao Dai[1,2,*]
[1]Department of Bioengineering, Northeastern University, Boston, MA, USA
[2]Lead contact
*Correspondence: g.dai@northeastern.edu
https://doi.org/10.1016/j.crmeth.2024.100732

MOTIVATION Direct conversion of patient fibroblasts toward vascular endothelial cells comprises a valuable source of cells for regenerative medicine and tissue engineering applications. Previous reprogramming approaches involving the transcription factor ETV2 retained limitations in programming efficiency and endothelial characteristics, such as eNOS expression. We aimed to develop an improved reprogramming approach combining ETV2 with SOX17 expression to help address these limitations.

SUMMARY

An autologous source of vascular endothelial cells (ECs) is valuable for vascular regeneration and tissue engineering without the concern of immune rejection. The transcription factor ETS variant 2 (ETV2) has been shown to directly convert patient fibroblasts into vascular EC-like cells. However, reprogramming efficiency is low and there are limitations in EC functions, such as eNOS expression. In this study, we directly reprogram adult human dermal fibroblasts into reprogrammed ECs (rECs) by overexpressing SOX17 in conjunction with ETV2. We find several advantages to rEC generation using this approach, including improved reprogramming efficiency, increased enrichment of EC genes, formation of large blood vessels carrying blood from the host, and, most importantly, expression of eNOS *in vivo*. From these results, we present an improved method to reprogram adult fibroblasts into functional ECs and posit ideas for the future that could potentially further improve the reprogramming process.

INTRODUCTION

Cardiovascular disease (CVD) is the leading cause of death worldwide and often results in substantially damaged vasculature.[1] These damaged blood vessels need to be replaced or repaired with functional vascular endothelial cells (ECs) so that the blood vessels can function properly. Therefore, a reliable source of ECs is essential for vascular regeneration and vascular tissue engineering. It is also desirable to obtain patient-specific ECs for these applications to avoid immune rejection, as ECs are in direct contact with immune cells in the blood. As such, transdifferentiation has arisen as a promising approach to convert a patient's own fibroblasts, which are easily obtainable, directly into endothelial-like cells. Previously, the overexpression of ETS variant 2 (ETV2) in fibroblasts led to the emergence of EC-like properties.[2,3] ETV2 is a transcription factor that is critical for the formation of vasculature during development.[4,5] The ETV2-reprogrammed fibroblasts developed certain endothelial properties, such as a typical endothelial cobblestone morphology and the expression of several endothelial-specific markers. The cells were able to maintain their commitment and functionality in culture. When implanted in mice, the cells were able to prevent necrosis and promote the regeneration of surrounding tissue. However, this approach is extremely inefficient, with less than 7% reprogramming efficiency, and a long conversion process with multiple sorting steps.[2] The reprogrammed cells also lack distinct human eNOS (endothelial nitric oxide synthase) expression, an important feature of vascular ECs.

SOX17, a member of the Sry-related high-mobility group box family of transcription factors, plays various major roles in all three germ layers, which indicates that the downstream effects of SOX17 are context dependent. In the endoderm, SOX17 plays a role in the developmental process and differentiation of the definitive endoderm (DE).[6] SOX17 has been shown to be vital to the formation of the DE, which later differentiates into lung, liver, pancreas, stomach, and gastrointestinal track cells.[7] Viotti et al. found that, in a *Sox17* mutant mouse model, embryos lacking Sox17 were deficient in the midgut and hindgut DE.[8] In the ectoderm, SOX17 contributes to oligodendrocyte progenitor cell (OPC) differentiation and maturation.[9] SOX17 is highly expressed in OPCs and peaks when the cells change phenotypes from bipolar to multipolar. Additionally, when SOX17 is downregulated, OPC proliferation increased, and when SOX17 is

overexpressed, OPC proliferation decreased, and myelin gene expression was enhanced.

In the mesoderm, SOX17 plays an important role in vascular development[10] and is highly expressed in arterial ECs, but not in venous ECs, from embryonic development all the way to adulthood.[11] In the artery, SOX17 seems critical for maintaining arterial functions, as a defect in SOX17 is correlated with pulmonary arterial hypertension.[12,13] Additionally, overexpressing SOX17 in venous ECs drives them to an arterial phenotype, and they begin to increase the expression of genes relating to arterial and tip cell identity.[14] SOX17 has other roles in the mesoderm, including hematopoiesis,[15,16] endocardium and cardiomyocyte differentiation,[17,18] and fibroblast-to-EC transdifferentiation.[19] Schachterle et al. investigated the role of SOX17 in murine amniotic-to-EC transdifferentiation.[20] They found that SOX17 increases the expression of morphogenesis genes and promotes integration of transplanted reprogrammed cells into injured vessels. Thus, SOX17 is critical for functional engraftment of endothelium. However, cells reprogrammed with SOX17 alone showed incomplete reprogramming.[20] This study uses amniotic cells, and it is expected that younger cells types are much easier to reprogram because they are at an earlier stage of the developmental hierarchy. However, the ability to convert adult fibroblasts in elderly patients is necessary because they are the predominant population that needs vascular regeneration treatments. Thus, developing a method to efficiently reprogram adult fibroblasts into functional ECs is vital to address this unmet clinical need.

Currently, the major obstacle in this field is the low reprogramming efficiency; if these cells are to be used in time-sensitive clinical applications, then the reprogramming process must be rapid and yield a large number of usable ECs. Thus, our work sought to improve the efficiency of the reprogramming process, as the current low efficiency hinders the chance that the cells see clinical use. To enhance reprogramming and better understand the process, we investigated the effects of inducing SOX17, a transcription factor that has been found to promote engraftment and drive an arterial EC phenotype, in conjunction with ETV2. By refining the reprogramming process, we are able to efficiently and rapidly generate a higher percentage of reprogrammed ECs (rECs) (~17.8% vs. 2%–10% reported in previous methods[2,3,21,22]) for use in tissue engineering and regenerative medicine applications.

RESULTS

Overexpression of ETV2 and SOX17 results in higher reprogramming efficiency than ETV2 alone

To control the timing and dose of the reprogramming process, we generated Tet-On lentiviruses to induce the expression of ETV2 and SOX17. Adult human dermal fibroblasts were transduced with the ETV2 lentivirus alone (ETV2-ECs), the SOX17 lentivirus alone (SOX17-ECs), or both the ETV2 and SOX17 lentiviruses (rECs). Both the ETV2 and SOX17 lentiviruses are Tet-On and only express their respective transcription factor in the presence of doxycycline. To confirm successful transduction of our cells and establish a dose-response curve, we treated the cells with varying amounts of doxycycline and for varying amounts of time (Figures 1A and 1B). The cells were cultured for 12 days, and RT-qPCR was used to measure the expression of ETV2 and SOX17 mRNA. We found that there was high expression of ETV2 and SOX17 when the cells were treated with 1,000 ng/mL doxycycline. Thus, we treated the transduced fibroblasts with 1,000 ng/mL doxycycline in all following experiments. We also stained the reprogrammed cells to further confirm expression of SOX17 and found that a large portion of our rECs express SOX17, while fibroblasts, ETV2-ECs, and human umbilical vein ECs (HUVECs) do not express any SOX17 (Figure S1). After induction of ETV2 and SOX17 in the cells, the expression of vascular endothelial cadherin (VE-CAD), CD31, and FLK1 all increased dramatically, ranging from hundreds to thousands of folds, in comparison to the fibroblast control. Additionally, we found that the height of VE-CAD and CD31 expression occurred at day 12 after induction with doxycycline (Figure 1B). Therefore, we evaluated the rECs at day 12 in all following experiments to determine how they compare to fibroblasts (negative control) and HUVECs. We used HUVECs as a positive control and the transduced fibroblasts with 0 ng/mL doxycycline as a negative control.

We evaluated the VE-CAD, CD31, and FLT1 mRNA expression of the ETV2-ECs, SOX17-ECs, and rECs (Figure 1C). We found that the rECs expressed significantly higher VE-CAD, CD31, and FLT1 than ETV2-ECs or SOX17-ECs. VE-CAD and FLT1 expression was higher than HUVECs. However, CD31 expression in rECs was still low when compared to HUVECs. The ETV2-ECs and SOX17-ECs were able to upregulate these markers as well but to a much lesser extent. We also used this reprogramming method to transdifferentiate two other fibroblast cells lines, an adult human lung fibroblast cell line (Figure S2A) and a different adult human dermal fibroblast cell line (Figure S2C), and found similar expression patterns. Lung rECs significantly upregulated VE-CAD over lung ETV2-ECs, whereas CD31 and FLT1 expression was similar. In the second dermal fibroblast cell line, the rECs significantly upregulated both VE-CAD and CD31 over ETV2-ECs, and FLT1 expression was similar. We also measured the relative mRNA expression of fibroblast-specific markers (TWIST2, PDGFRA) (Figure S3) and several venous (NRP2, NR2F2, TIE2, EPHB4) and arterial (NOTCH4, NRP1, DLL4, EFNB2, JAG1) EC markers (Figure S4). At the population level, rECs and ETV2-ECs had decreased expression of fibroblast markers (Figure S3). rECs had increased arterial marker expression and similar venous marker expression compared to ETV2-ECs (Figure S4A). We then sorted rECs to obtain a $CD31^+$ population and performed RT-qPCR to measure several venous and arterial EC markers to determine how they compare to HUVECs (Figure S4B). Interestingly, purified rECs had significantly upregulated arterial markers compared to HUVECs, while venous marker expression was roughly the same or lower than that of HUVECs, except for NRP2. Additionally, to evaluate if the rECs begin to take on and maintain an arterial phenotype during the reprogramming process, we stained for arterial protein EphrinB2 (Figure S4C). We found that the rECs strongly express EphrinB2 as early as day 6 and maintain expression at day 12, while HUVECs express low levels of EphrinB2, indicating that the overexpression of SOX17 is driving the rECs to express several arterial markers.

To confirm that these cells were correctly expressing the EC markers, we also performed immunocytochemistry to stain the

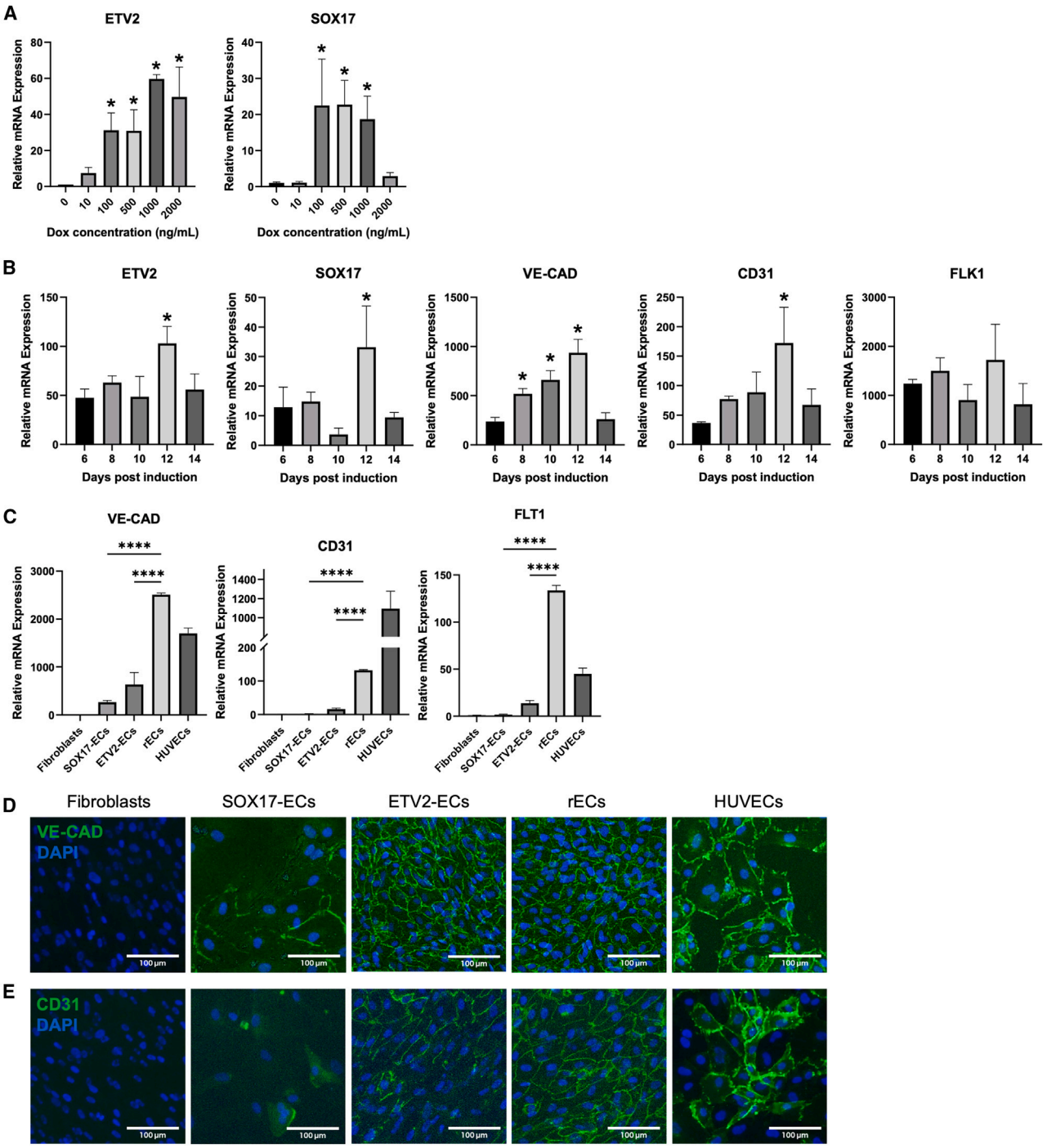

Figure 1. Human adult fibroblasts take on endothelial cell-like properties when reprogrammed with ETV2 and SOX17

ETV2 and SOX17 Tet-On-lentivirus-transduced fibroblasts were induced using doxycycline (dox).

(A) Relative mRNA expression of ETV2 and SOX17 in rECs at day 12.

(B) Relative mRNA expression of ETV2, SOX17, VE-CAD, CD31, and FLK1 in rECs cultured with 1,000 ng/mL dox at various time points. Significance shown compared to day 6 expression.

(C) Relative mRNA expression of EC markers VE-CAD, CD31, and FLT1 in fibroblasts, SOX17-ECs, ETV2-ECs, rECs, and HUVECs.

(D and E) Representative VE-CAD and CD31 stains (green) of the different cell types. RN18S served as an endogenous control for RT-qPCR, and values were normalized to fibroblasts. n = 3, one-way ANOVA, *$p < 0.05$ and ****$p < 0.0001$. Data presented as mean ± standard deviation.

cells for VE-CAD and CD31 (Figures 1D and 1E). The rECs showed spatial localization of both of these proteins at the cell-cell border, confirming a confluent monolayer of rECs. Similar stains were observed in ETV2-ECs; however, VE-CAD and CD31 were barely expressed in the SOX17-ECs, and their spatial localization was also incorrect. The stains showed some cytosolic fluorescence when VE-CAD and CD31 should only be expressed on the cell membrane. It should be noted that while the VE-CAD stain in the ETV2-ECs covers the entire image in the chosen area, VE-CAD was not uniformly expressed across the entire sample. Rather, there were clusters of cells not expressing VE-CAD (data not shown).

rECs acquire certain EC functions

After the preliminary work was successful, we moved to functional assays. rECs must perform as functional ECs in order to work effectively in regenerative medicine and tissue engineering. We quantified VE-CAD and CD31 protein expression; we quantified what percentage of the cell populations was expressing VE-CAD and CD31 using fluorescence-activated cell sorting (FACS) to analyze the VE-CAD$^+$ and CD31$^+$ populations (Figure 2A). Approximately 17.8% of rECs expressed CD31 and 63.2% of them expressed VE-CAD, which is higher than the ETV2-ECs, in which 10.7% of the ETV2-ECs expressed CD31 and 46.2% of them expressed VE-CAD, which aligns with previous studies.[2] We also used FACS to quantify the VE-CAD$^+$ and CD31$^+$ populations in the lung fibroblast cell line (Figure S2B) and the additional dermal fibroblast cell line (Figure S2D). The lung rECs had vastly more VE-CAD$^+$ cells than the lung ETV2-EC population (49.8% vs. 6.0%). The additional dermal rECs also had more VE-CAD$^+$ and CD31$^+$ cells than the ETV2-EC population (VE-CAD: 71.8% vs. 45.2%; CD31: 22.0% vs. 16.0%).

We also observed the morphological changes of our rECs over time (Figure 2B). The rECs transitioned from long, spindle-shaped cells into a typical EC cobblestone pattern as early as day 3 and became more complete by day 6. ETV2-ECs were unable to achieve a change in morphology until day 6, and the SOX17-ECs never changed morphology. With these preliminary assays completed, we moved to measure the rECs' ability to perform critical EC functions and exhibit EC features, such as the ability to uptake low-density lipoprotein (LDL), form tubules, and express von Willebrand factor (vWF). LDL uptake is a hallmark of ECs.[23,24] ECs internalize and degrade LDL from the bloodstream to maintain vascular homeostasis.[25] The rECs and ETV2-ECs were capable of uptaking LDL, as were the SOX17-ECs, albeit to a lesser extent (Figure 2C). We quantified the amount of LDL uptake across all of the groups and normalized it to cell count and found that both ETV2-ECs and rECs took up more LDL compared to HUVECs (Figure 2D). Additionally, because the SOX17-ECs did not perform well in all of the above assays, we decided to not proceed with characterizing them further.

We investigated the cells' ability to form tubules when cultured on Matrigel (Figure 2E). Fibroblasts were unable to form tubes and instead formed star-like structures. Both ETV2-ECs and rECs were able to form tubes, which resemble HUVECs. vWF is produced by ECs and serves to aid the blood clotting process.[26] We stained for vWF and found that both rECs and ETV2-ECs express vWF (Figure 2F). However, the ETV2-EC and rEC stains show that the vWF is likely not being fully expressed or formed properly, as the entire cytoplasm of these cells is not stained. In HUVECs, the entire cytoplasm is stained with vWF, along with distinct Weibel-Palade bodies, which is typical of ECs.[27] We also measured the relative mRNA expression of vWF and found that rECs express more vWF than ETV2-ECs (Figure 2G). However, this expression was still low when compared to HUVECs and could potentially be the reason that we do not see a distinct vWF and Weibel-Palade body stain in ETV2-ECs and rECs.

rECs respond to inflammatory and flow stimuli

We next examined inflammatory responses by treating the cells with 10 ng/mL of tumor necrosis factor α (TNF-α) for 6 h and then measured the expression of inflammatory adhesion molecules E-selectin (SELE), VCAM1, and ICAM1. We found that the rECs were able to respond to inflammatory stimuli by upregulating SELE, VCAM1, and ICAM1 compared to non-treated rECs but were unable to express VCAM1 and SELE to the extent of HUVECs (Figure 3A). The response of ETV2-ECs to inflammatory stimuli is comparable to rECs.

Next, we examined the rECs' and ETV2-ECs' response to flow stimuli after being fully reprogrammed. Cells were reprogrammed and subjected to 48 h of 5 dyn/cm^2 shear stress. We investigated morphology and upregulated genes (Figure 3B). In the presence of flow, the morphology of the fibroblasts is different than that of the ETV2-ECs, rECs, and HUVECs. Fibroblasts tend to be very long and spindle shaped, as expected. ETV2-ECs and rECs maintain the cobblestone morphology as seen in HUVECs. Interestingly, they do not show much alignment to flow direction. When these cells were harvested for RT-qPCR, it was found that rECs in flow conditions expressed slightly more KLF2 than ETV2-ECs in flow conditions (Figure 3C). Also, rECs in static and flow conditions expressed eNOS, while ETV2-ECs were unable to express any eNOS in either static or flow conditions. rECs under flow expressed significantly more eNOS than ETV2-ECs under flow. Additionally, rECs express significantly more eNOS while under flow compared to rECs cultured in static conditions. However, when the rECs were stained for eNOS protein, nothing was found in the stains (data not shown). We think that this is likely due to the fact that the low amount of eNOS mRNA is not sufficient to generate enough eNOS protein to be stained, as the eNOS gene expression, although upregulated, remains low compared to HUVECs (Figure 3C).

rECs are enriched in EC-specific genes

ETV2-ECs and rECs were reprogrammed and sorted into a CD31$^+$ population before isolating their RNA and sending it to Genewiz for RNA sequencing (RNA-seq). All of the data were processed using RStudio, iDEP.91 from South Dakota State University, and geneontology.org. We generated a gene heatmap of all of the differentially expressed genes (DEGs) of the fibroblasts, ETV2-ECs, rECs, and HUVECs (Figure 4A). Clustering analysis showed that ETV2-ECs clustered more closely with fibroblasts than rECs, while rECs clustered further away from fibroblasts than ETV2-ECs, showing more widespread genome expression changes as a result of the upregulation of SOX17 in conjunction with ETV2. Nevertheless, fibroblasts, ETV2-ECs, and rECs are

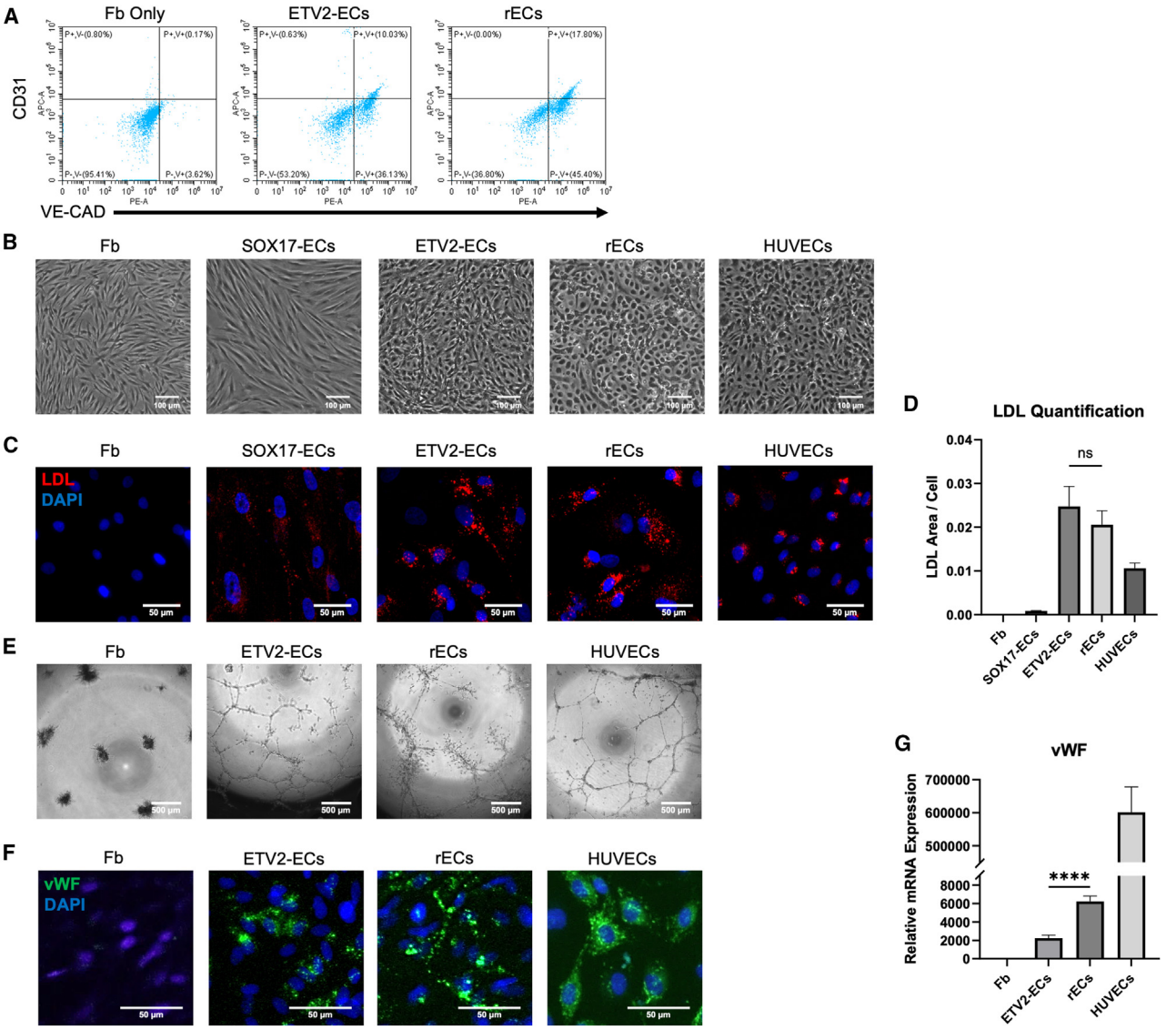

Figure 2. Reprogrammed cells were characterized using several functional assays to determine how well they mimic mature endothelial cells

(A) FACS was used to measure the percentage of cells in a population expressing VE-CAD and CD31.

(B) Representative bright-field images showing changes in morphology in the reprogrammed cell lines at day 6.

(C) Representative images of different types of cells uptaking and retaining low-density lipoprotein (LDL) after being treated with 10 μg/mL LDL for 4 h.

(D) Quantification of uptaken LDL in each group, normalized to cell count.

(E) Representative bright-field images of tubule formation when the reprogrammed cells were cultured on Matrigel.

(F) Representative images of von Willebrand factor (vWF) stains (green) of fibroblasts, ETV2-ECs, rECs, and HUVECs.

(G) Relative mRNA expression of vWF in fibroblasts, ETV2-ECs, rECs, and HUVECs. RN18S served as an endogenous control for RT-qPCR, and values were normalized to fibroblasts. n = 3, one-way ANOVA, ****$p < 0.0001$. Data presented as mean ± standard deviation.

still far away from HUVECs, suggesting that there is still room for improvement for cellular reprogramming to obtain desired cell types. However, when analyzing a heatmap focused on only EC-related genes, the difference between ETV2-ECs and rECs becomes more apparent (Figure 4B). rECs cluster closer to HUVECs, while ETV2-ECs cluster closer to fibroblasts. It is obvious from the heatmap that rECs were enriched in EC-specific gene expression, demonstrating significantly more upregulation of EC-specific genes than ETV2-ECs. We conducted a principal-component analysis of the different cell types using the DEGs and found that the ETV2-ECs clustered very tightly with fibroblasts, while the rECs were much further away (Figure 4C). However, both rECs and ETV2-ECs still cluster far away from HUVECs, again showing that there is room for improvement in the reprogramming process. The gene heatmap consisting of only fibroblast-related genes shows that rECs

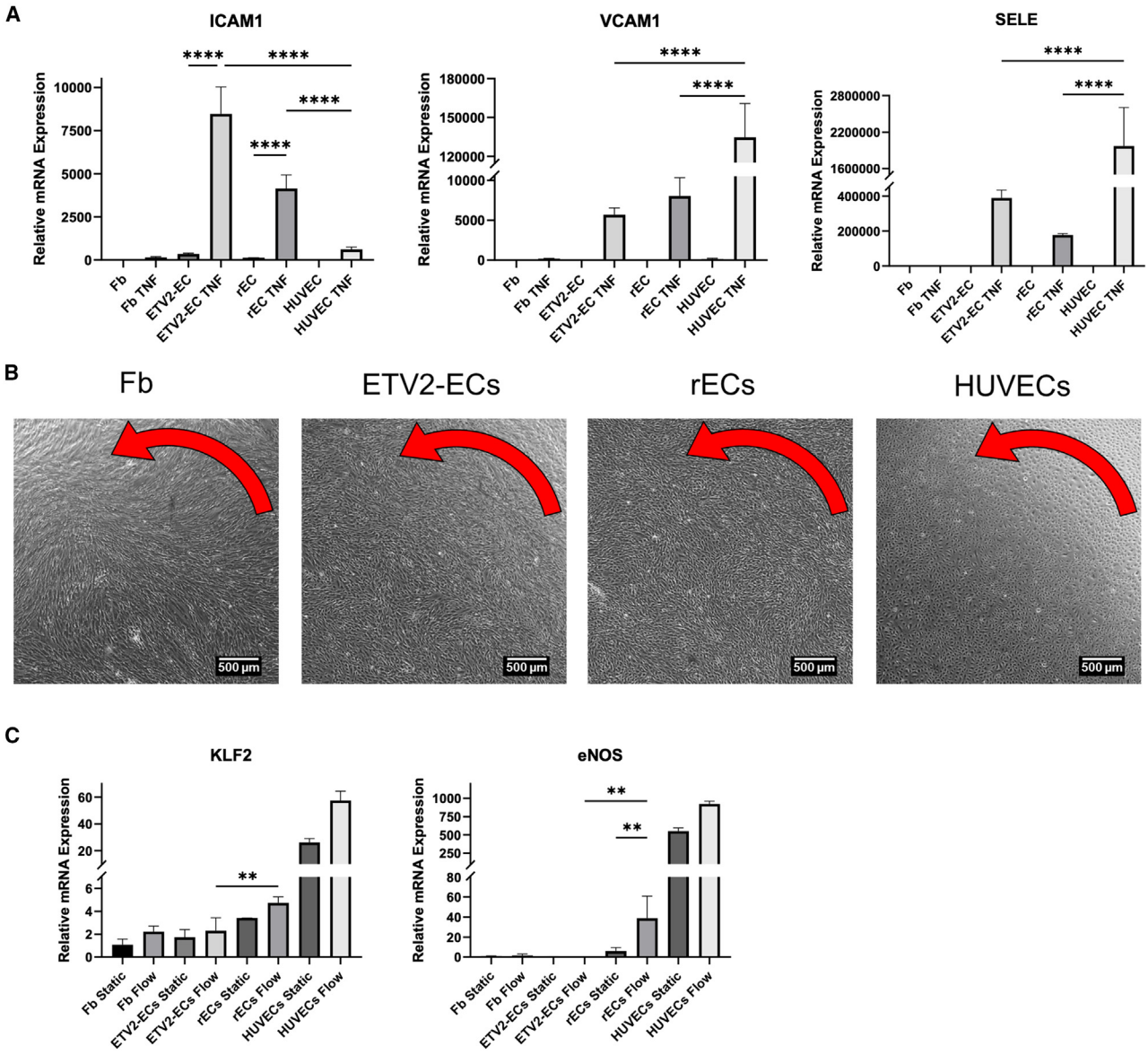

Figure 3. rECs respond to inflammatory and shear-stress stimuli

(A) Relative mRNA expression of inflammatory markers ICAM1, VCAM1, and E-selectin (SELE) after the cells were cultured with or without 10 ng/mL of tumor necrosis factor α (TNF-α) for 6 h.

(B) Cells maintain their morphology when under shear stress. Representative bright-field images for each cell type 48 h after onset of 5 dyn/cm^2 shear stress. Red arrow indicates direction of flow. ETV2-ECs and rECs were fully reprogrammed before being subjected to fluid flow.

(C) Relative mRNA expression of flow markers KLF2 and eNOS in fibroblasts, ETV2-ECs, rECs, and HUVECs under static and flow conditions. RN18S served as an endogenous control for RT-qPCR, and values were normalized to fibroblasts. n = 3, one-way ANOVA, **p < 0.01 and ****p < 0.0001. Data presented as mean ± standard deviation.

cluster with ETV2-ECs, both of which cluster more closely with fibroblasts than HUVECs (Figure S5).

Next, we clustered the top 2,000 DEGs into 5 clusters based on gene function (Figure 4D). The five different clusters focused on EC processes, cell adhesion, cell differentiation, tissue development, and neutrophil migration. rECs resemble HUVECs in their expression of genes relating to vascular development and angiogenesis, as compared to fibroblasts and ETV2-ECs, which have these genes downregulated. The fibroblasts, ETV2-ECs, and rECs show similar expression in the cell adhesion and tissue development clusters. The fibroblasts, ETV2-ECs, and rECs have low expression of cell adhesion genes compared to HUVECs, which form extremely tight monolayers. The fibroblasts, ETV2-ECs, and rECs have high expression of genes in the tissue development cluster compared to HUVECs, which align with their original purpose of forming connective tissue

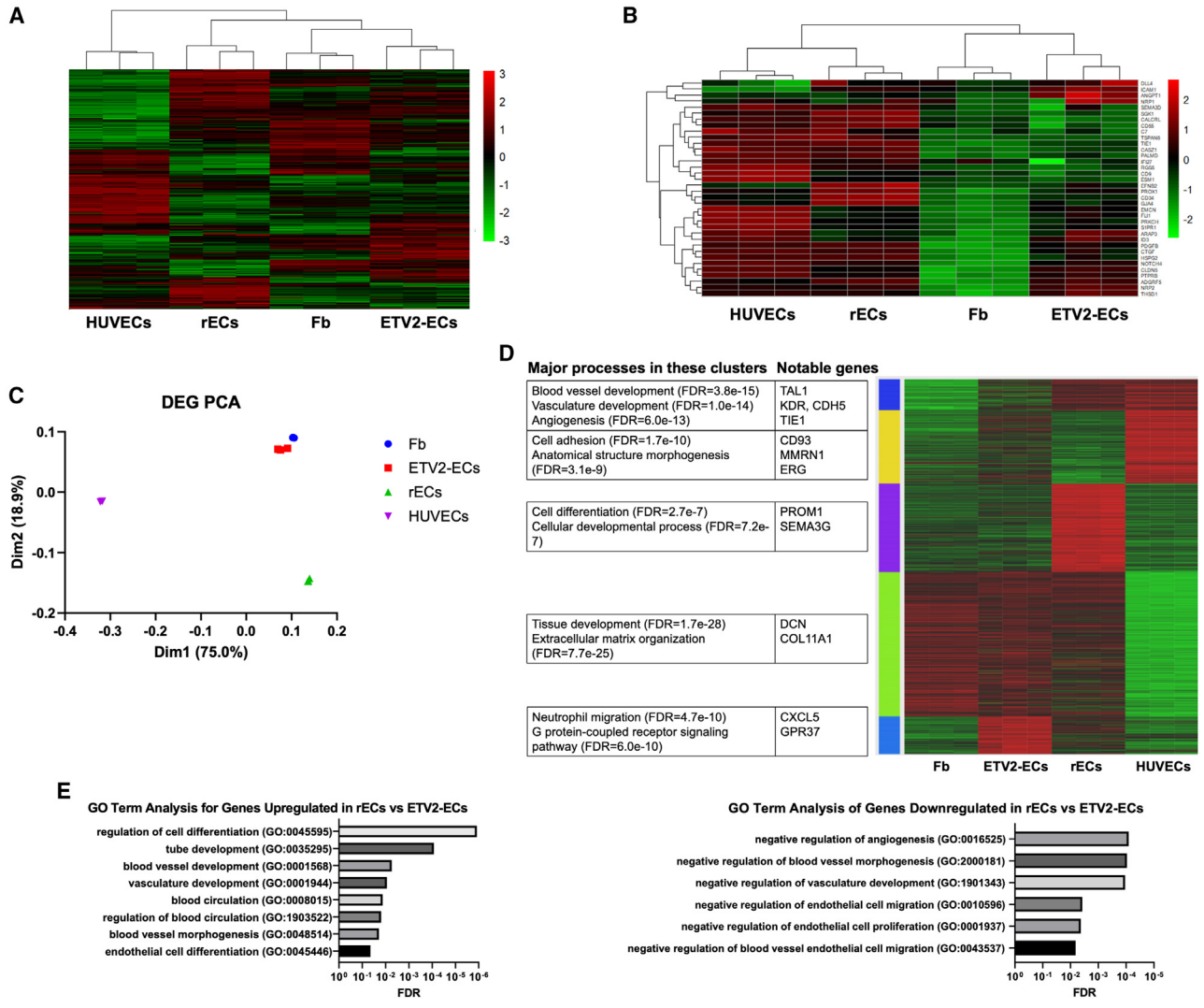

Figure 4. RNA sequencing was performed on fibroblasts, ETV2-ECs, rECs, and HUVECs

(A) Gene heatmap of the differentially expressed genes (DEGs) of each cell type.

(B) Gene heatmap of only endothelial-specific genes of each cell type.

(C) Principal-component analysis (PCA) of each cell type when analyzing DEGs.

(D) Clustering of the top 2,000 DEGs into 5 clusters, labeled with the major functions and genes in each cluster.

(E) Gene Ontology (GO) term analysis of genes upregulated in rECs compared to ETV2-ECs (left) and downregulated in rECs compared to ETV2-ECs (right).

and depositing extracellular matrix. Interestingly, genes relating to cell differentiation are highly upregulated in rECs compared to ETV2-ECs, showing that reprogramming with ETV2 and SOX17 simultaneously results in more widespread cellular differentiation.

Next, we performed a Gene Ontology (GO) term analysis on the DEGs. Here, we compared gene expression in rECs to ETV2-ECs. We separated upregulated (Figure 4E, left) and downregulated genes (Figure 4E, right) to identify specific processes that are occurring in the rECs. We found that several EC gene sets were significantly expressed in the rECs compared to the ETV2-ECs, notably the regulation of cell differentiation, tube development, and blood vessel morphology and vasculature development. Many negative regulatory pathways were also significantly downregulated in rECs compared to ETV2-ECs, including the negative regulation of angiogenesis, blood vessel morphogenesis, and vasculature development, which suggests strong upregulation of vascular development and angiogenesis-related processes in the rECs.

rECs undergo vasculogenesis *in vivo*

To evaluate EC functions *in vivo*, fibroblasts, ETV2-ECs, rECs, and HUVECs were tested in an *in vivo* GelTrex plug assay to visualize the cells' ability to undergo vasculogenesis. Briefly, ETV2-ECs and rECs were reprogrammed and CD31^{+} sorted before being resuspended in GelTrex, a Matrigel alternative, and injected into the abdominal flank of mice (sham [no cells], fibroblasts, and HUVECs n = 3; ETV2-ECs, rECs n = 4) (Figure 5A). The plugs

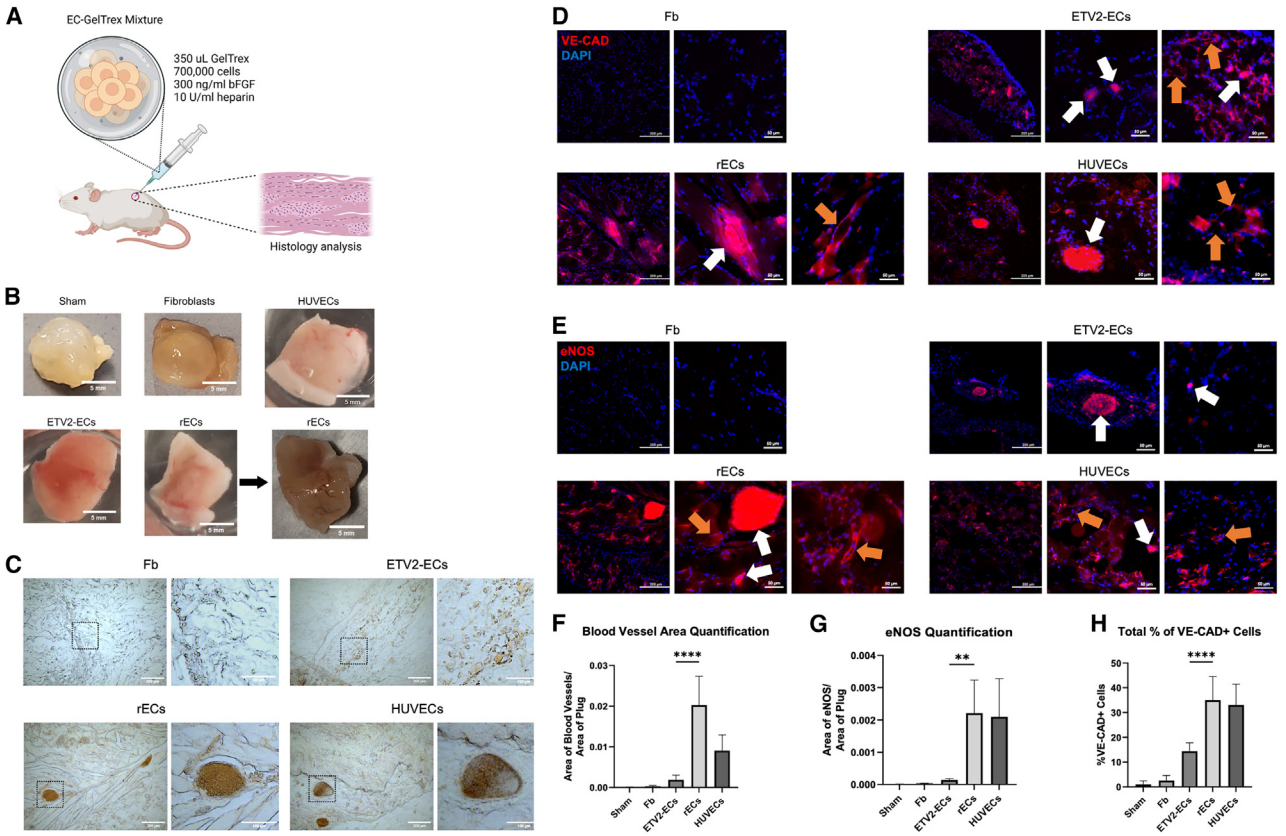

Figure 5. *In vivo* vasculogenesis assay

(A) Schematic of the GelTrex plug assay. A sham (no cells, n = 3), fibroblasts (n = 3), ETV2-ECs (n = 4), rECs (n = 4), or HUVECs (n = 3) suspended in GelTrex were injected subcutaneously into the flank of nude mice, cultured for 14 days, and then excised.

(B) Representative image of an excised plug from each treatment group.

(C) Representative bright-field image of plugs after they were cryosectioned. Red/orange areas indicate erythrocytes and blood vessels.

(D and E) Representative images of human VE-CAD (red) and human eNOS (red) stains of the plugs. Round, high-intensity areas signify erythrocytes. White arrows indicate blood vessel lumen filled with red blood cells. Orange arrows indicate hollow open lumen.

(F) Quantification of blood vessel area found in each treatment group.

(G) Quantification of human eNOS found in each treatment group.

(H) Quantification of total percentage of $VECAD^{+}$ cells in each treatment group. One-way ANOVA, $^{**}p < 0.01$ and $^{****}p < 0.0001$. Data presented as mean ± standard deviation.

were left in the mice for 14 days, at which point they were excised and cryosectioned for immunohistochemistry. The newly excised plugs were photographed, and blood could be seen in the ETV2-EC, rEC, and HUVEC samples (Figure 5B). When the rEC samples were trimmed, the blood vessels in the plug could be seen with the naked eye. After cryosectioning, the plug slices were imaged using a bright-field microscope (Figure 5C). The rEC and HUVEC samples had clear cross-sections of large blood vessels carrying red blood cells, while ETV2-EC samples had only small blood vessels. Both the sham and fibroblast control samples had no blood vessels. The total blood vessel area compared to the entire area of the plugs was quantified, and it was found that the rEC samples had the largest percentage of blood vessel area and significantly more blood vessel area than ETV2-ECs (Figure 5F).

Next, the cryosectioned plugs were stained for human VE-CAD and human eNOS (Figures 5D and 5E). The ETV2-EC, rEC, and HUVEC samples all showed VE-CAD expression. The bright, circular regions in the stains represent erythrocytes, as they absorb and retain the antibodies even after extensive washing. The rEC VE-CAD stain showed a blood vessel completely surrounded by cells expressing human VE-CAD, along with satellite VE-CAD expression around other, smaller blood vessels. We found that the ETV2-EC, rEC, and HUVEC samples contained both blood vessel lumen filled with red blood cells as well as open, hollow lumen without red blood cells. In the eNOS stains, it is clear that the rEC and HUVEC samples express eNOS; however, the ETV2-ECs either express none or very little. The ETV2-EC stain shows only erythrocyte antibody absorption and some background and does not have a network that is seen in the rEC and HUVEC stains. We quantified the eNOS expression in each group, excluding the erythrocyte fluorescence (Figure 5G). The rECs had similar eNOS expression compared to HUVECs, and it was also significantly higher than ETV2-ECs. We also quantified the number of $VE\text{-}CAD^{+}$ cells in each group to estimate how many of the

implanted cells matured to become ECs (Figure 5H). There was significantly more VE-CAD$^+$ cells in the rEC plugs compared to the ETV2-EC plugs. The rEC plugs had similar levels of VE-CAD$^+$ cells to the HUVEC plugs.

DISCUSSION

A reliable source of patient-specific functional ECs will be extremely valuable for cardiovascular regenerative medicine and tissue engineering applications. However, current methods of reprogramming ECs are all very inefficient, and some lack functional outcomes. Our study showed that reprogramming adult fibroblasts into ECs using both ETV2 and SOX17 provides advantages over ETV2 alone. ETV2 is well established as a master transcription factor for EC fate,[5] and SOX17 helps improve the engraftment of newly formed blood vessels[20] and drives an arterial phenotype in ECs.[14] Together, these transcription factors generate more mature rECs at a higher efficiency than ETV2 alone. The ETV2-ECs performed very similarly to those established in previous works.[2,3,21,22] Thus, it appears that SOX17 directly aids the reprogramming process.

The transdifferentiation process is similar to induced pluripotent stem cell (iPSC) reprogramming in many ways but also comes with several key differences. Both processes begin with one cell type, commonly fibroblasts, and reprograms them into a final cell type that matches a desired physiological phenotype. However, the steps to get there are different. iPSC reprogramming must first reprogram cells into an iPSC state by increasing the expression of key genes, after which they can be differentiated into the desired cell type.[28] The reprogramming process is long and takes roughly 3-4 weeks to achieve clonal iPSC expansion, with an incredibly low efficiency that lies between 0.01% and 1%.[29,30] After this, the iPSCs will need to be expanded and differentiated into ECs, which take another several weeks. In contrast, transdifferentiation does not require this step and is usually a much more rapid process than iPSC reprogramming. For example, our data show the emergence of EC properties in as few as 6 days, with 12-day-old rECs capable of forming perfused blood vessels *in vivo*. The best methods for generating usable patient-specific ECs from fibroblasts using iPSC reprogramming take roughly 4–5 weeks.[31] If one wishes to bypass the inefficient dedifferentiation process and instead use the readily available allogenic iPSCs to create ECs, then there is a risk of immune rejection, whereas the transdifferentiation method can produce autologous cells more quickly. Once a stable iPSC line is created, EC differentiation is typically driven using small molecules and growth factors.[32,33] In transdifferentiation, EC reprogramming is driven using a mix of overexpressed transcription factors and small molecules.[2,21,22,34] In summary, full iPSC reprogramming is time consuming, costly, and inefficient, while transdifferentiation can occur much more rapidly.

While iPSC differentiation and transdifferentiation take different reprogramming routes, our rECs perform similarly to ECs derived from iPSCs.[31,35–37] However, it should be noted that fibroblast-to-EC transdifferentiation is incredibly infantile compared to iPSC-derived ECs. The first major success of EC transdifferentiation arose in 2015 with the emergence of ETV2 as a target of interest,[2,3] while iPSC-ECs have been researched since the discovery of iPSCs in 2006,[28] with knowledge of embryonic stem cell differentiation dating back to 1992.[38,39] iPSC-EC differentiation is met with greatly varying levels of efficiency (6%–16%,[35] 18%,[37] >60%[31]), with higher efficiencies coming out in more recent years.[32,33] These iPSC-ECs can express key EC proteins VE-CAD and CD31, as well as vWF. They also take up and retain LDL, respond to inflammatory stimuli, and form tubules when cultured on Matrigel.[31,35,37]

Our rECs are also able to exhibit these characteristics. Additionally, iPSC-ECs can be directed toward an arterial phenotype by culturing them with VEGF and cAMP,[35] similar to how SOX17 can be used to drive arterial EC transdifferentiation.[14] It would be interesting to see if these small molecules play a role in determining arteriovenous identity in transdifferentiation or even make the overall reprogramming process more efficient. However, the main difference between iPSC-ECs and rECs is the expression of eNOS. iPSC-ECs are able to produce detectable eNOS proteins *in vitro,*[35,37] whereas our rECs or ETV2-ECs failed to do so. Despite not having eNOS expression *in vitro*, rECs start to express eNOS *in vivo*. The field of EC transdifferentiation is still very new, and more steps are being taken to further improve the reprogramming process and generate more robust rECs. There are many ideas, and we postulate assays that would be insightful to further characterize the rECs and identify how they can be enhanced, whether it be discovering small molecules that help reprogramming or using single-cell RNA-seq (scRNA-seq) to recognize and address shortcomings in the transdifferentiation process.

SOX17 has many different roles across all three germ layers, indicating that its function is context dependent.[6–9,11,14] We originally theorized that the overexpression of SOX17 would lead to a more arterial rEC population, and our data support this hypothesis. We believe that the rECs resemble arterial ECs following the induction of SOX17 because a purified population of rECs significantly upregulate arterial markers compared to HUVECs and ETV2-ECs, while venous markers are not significantly different, which also occurs when HUVECs overexpress SOX17.[14] We have seen that many of the rECs express the arterial protein EphrinB2, further supporting that the rECs express some arterial markers. There are some rECs that do not express EphrinB2; these could potentially be a venous phenotype or un-transdifferentiated cells. While it seems that the predominant subpopulation of the rECs is comprised of arterial ECs, there is likely some heterogenicity in the rEC population, as seen by the simultaneous expression of both venous and arterial markers. This phenomenon could potentially be due to the fact that the rECs are derived from fibroblasts, and fibroblasts are typically heterogeneous.[40] In the future, it would be very interesting to further isolate and characterize the rEC subpopulations.

Aside from driving an arterial phenotype, SOX17 also seems to have a contextual role in the transdifferentiation process. The RNA-seq data demonstrated that SOX17 induces widespread changes to genes related to cell differentiation, which are unrelated to arterial or venous differentiation, implying that SOX17 also augments the reprogramming process in the context of transdifferentiation. Therefore, the role of SOX17 in fibroblast-to-EC transdifferentiation appears to be both similar to and different from its role in ECs.

When we performed the *in vivo* GelTrex plug assay, we found that the fibroblast group failed to recruit mouse blood vessels. There was little to no blood vessel formation in the fibroblast group, where fibroblasts were thought to function to recruit blood vessel infiltration into the plug through the stimulation of angiogenic pathways. A large part of the formation of blood vessels in the ETV2-EC, rEC, and HUVEC groups comes from vasculogenesis, whereby the ECs in these groups organize to form vasculature; however, the fibroblast group lacks the cell source needed to undergo vasculogenesis. Additionally, the fibroblasts in the plug may not produce strong enough pro-angiogenic signals to promote mouse vessel infiltration into the plug. We implanted cells at a density of 2 million cells/mL, whereas typical physiological cell density is between 1 and 3 billion cells/mL. Therefore, our cell density is roughly 3 orders of magnitude lower than physiological cell density, which decreases the activity of many cell signaling pathways due to a very low amount of signaling molecules and cascades compared to physiological conditions. Our findings are also consistent with previous ETV2-EC and iPSC-EC studies. Lee et al. showed that fibroblasts do not produce significantly more blood vessels than a PBS sham in a hindlimb ischemia model (Figure 7D in Lee et al.).[3] In an *in vivo* Matrigel plug, Margariti et al. showed that fibroblast plugs do not form capillary-like structures (Figure 1J in Margariti et al.), nor do they express EC markers (Figure 2 in Margariti et al.).[41]

Overall, we see that the simultaneous induction of ETV2 and SOX17 improved the EC reprogramming efficiency and functional outcomes. Nevertheless, rECs are still far from mature vascular ECs in terms of gene expression profile and have a shortage of certain EC functions such as low KLF2 and eNOS expression in response to flow conditions, suggesting that there is still room for improvement. Our work established a baseline for future improvement. Previous studies have shown that the temporal control of transcription factors and small molecules plays a major role in both fibroblast-to-EC transdifferentiation and EC differentiation from iPSCs. It would be interesting to test out different timescales of ETV2 and SOX17 induction. Because SOX17 is expressed at a later time point than ETV2 in the development of ECs in physiological conditions, sequential overexpression of ETV2 followed by overexpression of SOX17 could improve the reprogramming process, as it better mimics *in vivo* conditions.[11]

Additionally, scRNA-seq could provide incredibly valuable insight into the reprogramming process. We discussed that the rECs likely form a heterogeneous population and that scRNA-seq would allow us to discover and characterize each of the present subpopulations.[42] Interestingly, not many transdifferentiation studies perform scRNA-seq on their reprogrammed cell lines.[34] The information gleaned from scRNA-seq could completely revolutionize transdifferentiation as a whole, as it reveals major signaling pathways that are lacking in the reprogrammed cells, which could be targeted to improve the reprogramming process.[43] scRNA-seq could also be used to analyze reprogrammed cells at different time points throughout the reprogramming process to visualize the cell-state transition from the original cell type into the final cell type.[44]

In summary, we were able to improve the reprogramming of adult fibroblasts toward ECs by simultaneously overexpressing ETV2 and SOX17. These rECs outperform ETV2-ECs in many functional aspects, which include higher reprogramming efficiency, being enriched in more EC genes, and expressing eNOS in response to flow. When the rECs were injected subcutaneously into mice, they were able to undergo vasculogenesis, producing new blood vessels that connect with the mouse's circulation and were perfused and capable of expressing human eNOS. Overall, we show that reprogramming fibroblasts into ECs using ETV2 and SOX17 is more efficient and generates better functional outcomes than reprogramming with ETV2 alone.

Limitations of the study

In this study, we only evaluated the functional outcomes at 12 days of reprogramming. It is unknown whether the reprogrammed cells acquire a stable EC phenotype and if the sorted rECs can be further expanded while still maintaining the key EC functions in culture. It is also unknown whether the reprogramming factors need to be turned on consistently or can be safely turned off after reprogramming. Given the dynamic state of cellular reprogramming, it is likely that the EC phenotype is continuously drifting in culture, which makes it difficult to predict what is the best timing to use these cells for clinical translation. Previously, it was observed that ETV2-ECs gradually lose the EC phenotype and that the second phase induction at the later time point is necessary to induce EC functions.[2] In the future, the epigenetic memory and the stability of the EC phenotypes need to be further studied.

Another limitation of the study is that both ETV2 and SOX17 are under the doxycycline-inducible lentivirus with the same antibiotic selection marker. This has certain limitations, as ETV2 and SOX17 can only be turned on or off at the same time, and the same antibiotic selection marker cannot guarantee 100% transfection of both ETV2 and SOX17, which leads to heterogeneous cell populations with some cells only expressing one transcription factor. Moving forward, bicistronic plasmids could be designed so that we can achieve a 100% transfection rate for both and independently control the precise timing of ETV2 and SOX17 induction to better mimic the ETV2 and SOX17 expression timeline during native vascular development.

One potential concern of this work is using lentiviruses for gene delivery. These lentiviruses pose possible health concerns when translated to clinical work, but we are currently in the process of moving away from exogenous overexpression and transitioning toward transient endogenous upregulation using CRISPR/dCas9 or modified RNA-based technologies[45] to target and upregulate ETV2 and SOX17. It is also proposed that CRISPR/dCas9 allows for more complete reprogramming by targeting endogenous genes.[46] Thus, we can use CRISPR to transiently upregulate ETV2 and SOX17 or use RNA technology to directly deliver ETV2/SOX17 RNAs to reprogram the fibroblasts without the need for lentiviruses.

We investigated how many implanted cells commit to an EC lineage by measuring the number of human VE-CAD$^+$ cells in each plug group. However, we did not fluorescently label our rECs before implanting them in the mice, in order to preserve all fluorescent channels for flexible downstream antibody staining. This limits our ability to track the cell fate of input cells. In the future, it would be beneficial to repeat this experiment but

to label the cells so that we can trace their progression and final phenotypic states in the mouse. This would allow us to precisely determine the percentage of rECs that form perfused vasculature and the percentage of failed rECs *in vivo*.

Despite improvement over ETV2-ECs, the rECs still have significant limitations, when compared to mature ECs, such as low CD31 expression, low KLF2 and eNOS expression in response to flow, low vWF expression and no Weibel-Palade body stain, and low E-selectin and VCAM-1 expression in response to inflammatory stimuli. The RNA-seq analysis confirmed that rECs, although enriched in more EC genes, are still far away from mature ECs, showing widespread gene expression pattern from HUVECs, raising the question of whether the rECs are *bona fide* vascular ECs. *In vivo*, although we observed that rECs are able to form vascular network carrying the host's blood and start to express eNOS, we also observed that some cells in the plugs seemed to form clumps, separate from the larger blood vessels. The heterogenicity described above could result in a subpopulation of reprogrammed cells that do not function properly and instead form clumps. Interestingly, our ETV2-ECs seemed to clump together more than those previously established and validated in a similar mouse model.[2] In that study, the percentage of $CD31^+$ cells is comparable to our ETV2-ECs. The *in vivo* evaluation is done at day 28, while ours is at day 14. Also, they did not perform flow-inducible KLF2 and eNOS measurements, so it is difficult to compare functional outcomes directly. However, it is important to note that we do not know the age of the cells used in the previous study. When the same method of ETV2 is applied in our study, which use fibroblasts from a 59-year-old donor, the ETV2-ECs data here is less promising than those previously published. It is possible that cells of different ages have different abilities to be reprogrammed. As cells age, their ability to function properly and, therefore, undergo reprogramming is also inhibited.[47] Therefore, some previous works that showed successful reprogramming using younger cells need to be re-examined to see if they can work efficiently on older cells. In the future, more work needs to be done specifically on improving the reprogramming efficiency of cells from elderly patients, as they are the predominant population that need the vascular therapy the most.

STAR★METHODS

Detailed methods are provided in the online version of this paper and include the following:

- KEY RESOURCES TABLE
- RESOURCE AVAILABILITY
  - Lead contact
  - Materials availability
  - Data and code availability
- EXPERIMENTAL MODEL AND SUBJECT DETAILS
  - Fibroblast culture and transduction
  - Endothelial cell culture
  - Fibroblast to endothelial cell transdifferentiation
  - Mice
- METHOD DETAILS
  - Quantitative Reverse Transcriptase Polymerase Chain Reaction (RT-qPCR)
  - Magnetic-activated cell sorting (MACS)
  - 2D immunocytochemistry
  - Brightfield and fluorescent microscopy
  - Fluorescent-activated cell sorting (FACS)
  - Low-density lipoprotein (LDL) uptake
  - Matrigel tubule formation
  - Inflammatory stimulus response
  - Reprogramming under flow
  - RNA-seq data analysis
  - *In vivo* GelTrex plug assay
- QUANTIFICATION AND STATISTICAL ANALYSIS

SUPPLEMENTAL INFORMATION

Supplemental information can be found online at https://doi.org/10.1016/j.crmeth.2024.100732.

ACKNOWLEDGMENTS

We would like to acknowledge the Institute for Chemical Imaging of Living Systems at Northeastern University for their assistance during the imaging process. All illustrations were generated with BioRender.com. This work was funded by the National Institutes of Health grants R01NS107462, R01HL162908, and R21NS121736; Department of Defense Discovery Award PR210332; and American Heart Association 19IPLOI34760604 and NASA 21-3DTMPS_2-0037.

AUTHOR CONTRIBUTIONS

The study was conceptualized by A.G. and G.D. All experiments were performed by A.G. The manuscript was written by A.G. and G.D.

DECLARATION OF INTERESTS

The authors declare no competing interests.

Received: July 27, 2023
Revised: November 7, 2023
Accepted: February 23, 2024
Published: March 18, 2024

REFERENCES

1. Martin, S.S., Aday, A.W., Almarzooq, Z.I., Anderson, C.A.M., Arora, P., Avery, C.L., Baker-Smith, C.M., Barone Gibbs, B., Beaton, A.Z., Boehme, A.K., et al. (2024). 2024 Heart Disease and Stroke Statistics: A Report of US and Global Data From the American Heart Association. Circulation *149*, e347–e913. https://doi.org/10.1161/CIR.0000000000001209.
2. Morita, R., Suzuki, M., Kasahara, H., Shimizu, N., Shichita, T., Sekiya, T., Kimura, A., Sasaki, K.i., Yasukawa, H., and Yoshimura, A. (2015). ETS transcription factor ETV2 directly converts human fibroblasts into functional endothelial cells. Proc. Natl. Acad. Sci. USA *112*, 160–165. https://doi.org/10.1073/pnas.1413234112.
3. Lee, S., Park, C., Han, J.W., Kim, J.Y., Cho, K., Kim, E.J., Kim, S., Lee, S.J., Oh, S.Y., Tanaka, Y., et al. (2017). Direct Reprogramming of Human Dermal Fibroblasts Into Endothelial Cells Using ER71/ETV2. Circ. Res. *120*, 848–861. https://doi.org/10.1161/CIRCRESAHA.116.309833.
4. Lammerts van Bueren, K., and Black, B.L. (2012). Regulation of endothelial and hematopoietic development by the ETS transcription factor Etv2. Curr. Opin. Hematol. *19*, 199–205. https://doi.org/10.1097/MOH.0b013e3283523e07.

5. Oh, S.Y., Kim, J.Y., and Park, C. (2015). The ETS Factor, ETV2: a Master Regulator for Vascular Endothelial Cell Development. Mol. Cells *38*, 1029–1036. https://doi.org/10.14348/molcells.2015.0331.

6. Burtscher, I., Barkey, W., Schwarzfischer, M., Theis, F.J., and Lickert, H. (2012). The Sox17-mCherry fusion mouse line allows visualization of endoderm and vascular endothelial development. Genesis *50*, 496–505. https://doi.org/10.1002/dvg.20829.

7. Kanai-Azuma, M., Kanai, Y., Gad, J.M., Tajima, Y., Taya, C., Kurohmaru, M., Sanai, Y., Yonekawa, H., Yazaki, K., Tam, P.P.L., and Hayashi, Y. (2002). Depletion of definitive gut endoderm in Sox17-null mutant mice. Development *129*, 2367–2379. https://doi.org/10.1242/dev.129.10.2367.

8. Viotti, M., Nowotschin, S., and Hadjantonakis, A.K. (2014). SOX17 links gut endoderm morphogenesis and germ layer segregation. Nat. Cell Biol. *16*, 1146–1156. https://doi.org/10.1038/ncb3070.

9. Sohn, J., Natale, J., Chew, L.J., Belachew, S., Cheng, Y., Aguirre, A., Lytle, J., Nait-Oumesmar, B., Kerninon, C., Kanai-Azuma, M., et al. (2006). Identification of Sox17 as a transcription factor that regulates oligodendrocyte development. J. Neurosci. *26*, 9722–9735. https://doi.org/10.1523/JNEUROSCI.1716-06.2006.

10. Zhou, Y., Williams, J., Smallwood, P.M., and Nathans, J. (2015). Sox7, Sox17, and Sox18 Cooperatively Regulate Vascular Development in the Mouse Retina. PLoS One *10*, e0143650. https://doi.org/10.1371/journal.pone.0143650.

11. Corada, M., Orsenigo, F., Morini, M.F., Pitulescu, M.E., Bhat, G., Nyqvist, D., Breviario, F., Conti, V., Briot, A., Iruela-Arispe, M.L., et al. (2013). Sox17 is indispensable for acquisition and maintenance of arterial identity. Nat. Commun. *4*, 2609. https://doi.org/10.1038/ncomms3609.

12. Park, C.S., Kim, S.H., Yang, H.Y., Kim, J.H., Schermuly, R.T., Cho, Y.S., Kang, H., Park, J.H., Lee, E., Park, H., et al. (2022). Sox17 Deficiency Promotes Pulmonary Arterial Hypertension via HGF/c-Met Signaling. Circ. Res. *131*, 792–806. https://doi.org/10.1161/CIRCRESAHA.122.320845.

13. Zhu, N., Welch, C.L., Wang, J., Allen, P.M., Gonzaga-Jauregui, C., Ma, L., King, A.K., Krishnan, U., Rosenzweig, E.B., Ivy, D.D., et al. (2018). Rare variants in SOX17 are associated with pulmonary arterial hypertension with congenital heart disease. Genome Med. *10*, 56. https://doi.org/10.1186/s13073-018-0566-x.

14. Kim, D., Grath, A., Lu, Y.W., Chung, K., Winkelman, M., Schwarz, J.J., and Dai, G. (2023). Sox17 mediates adult arterial endothelial cell adaptation to hemodynamics. Biomaterials *293*, 121946. https://doi.org/10.1016/j.biomaterials.2022.121946.

15. Kim, I., Saunders, T.L., and Morrison, S.J. (2007). Sox17 dependence distinguishes the transcriptional regulation of fetal from adult hematopoietic stem cells. Cell *130*, 470–483. https://doi.org/10.1016/j.cell.2007.06.011.

16. Clarke, R.L., Yzaguirre, A.D., Yashiro-Ohtani, Y., Bondue, A., Blanpain, C., Pear, W.S., Speck, N.A., and Keller, G. (2013). The expression of Sox17 identifies and regulates haemogenic endothelium. Nat. Cell Biol. *15*, 502–510. https://doi.org/10.1038/ncb2724.

17. Saba, R., Kitajima, K., Rainbow, L., Engert, S., Uemura, M., Ishida, H., Kokkinopoulos, I., Shintani, Y., Miyagawa, S., Kanai, Y., et al. (2019). Endocardium differentiation through Sox17 expression in endocardium precursor cells regulates heart development in mice. Sci. Rep. *9*, 11953. https://doi.org/10.1038/s41598-019-48321-y.

18. Liu, Y., Asakura, M., Inoue, H., Nakamura, T., Sano, M., Niu, Z., Chen, M., Schwartz, R.J., and Schneider, M.D. (2007). Sox17 is essential for the specification of cardiac mesoderm in embryonic stem cells. Proc. Natl. Acad. Sci. USA *104*, 3859–3864. https://doi.org/10.1073/pnas.0609100104.

19. Zhang, L., Jambusaria, A., Hong, Z., Marsboom, G., Toth, P.T., Herbert, B.S., Malik, A.B., and Rehman, J. (2017). SOX17 Regulates Conversion of Human Fibroblasts Into Endothelial Cells and Erythroblasts by Dedifferentiation Into CD34(+) Progenitor Cells. Circulation *135*, 2505–2523. https://doi.org/10.1161/CIRCULATIONAHA.116.025722.

20. Schachterle, W., Badwe, C.R., Palikuqi, B., Kunar, B., Ginsberg, M., Lis, R., Yokoyama, M., Elemento, O., Scandura, J.M., and Rafii, S. (2017). Sox17 drives functional engraftment of endothelium converted from non-vascular cells. Nat. Commun. *8*, 13963. https://doi.org/10.1038/ncomms13963.

21. Sayed, N., Wong, W.T., Ospino, F., Meng, S., Lee, J., Jha, A., Dexheimer, P., Aronow, B.J., and Cooke, J.P. (2015). Transdifferentiation of human fibroblasts to endothelial cells: role of innate immunity. Circulation *131*, 300–309. https://doi.org/10.1161/CIRCULATIONAHA.113.007394.

22. Van Pham, P., Vu, N.B., Nguyen, H.T., Huynh, O.T., and Truong, M.T.H. (2016). Significant improvement of direct reprogramming efficacy of fibroblasts into progenitor endothelial cells by ETV2 and hypoxia. Stem Cell Res. Ther. *7*, 104. https://doi.org/10.1186/s13287-016-0368-2.

23. Chopra, H., Hung, M.K., Kwong, D.L., Zhang, C.F., and Pow, E.H.N. (2018). Insights into Endothelial Progenitor Cells: Origin, Classification, Potentials, and Prospects. Stem Cells Int. *2018*, 9847015. https://doi.org/10.1155/2018/9847015.

24. Voyta, J.C., Via, D.P., Butterfield, C.E., and Zetter, B.R. (1984). Identification and isolation of endothelial cells based on their increased uptake of acetylated-low density lipoprotein. J. Cell Biol. *99*, 2034–2040. https://doi.org/10.1083/jcb.99.6.2034.

25. Vogel, R.A. (1999). Cholesterol lowering and endothelial function. Am. J. Med. *107*, 479–487. https://doi.org/10.1016/s0002-9343(99)00261-2.

26. Dmitrieva, N.I., and Burg, M.B. (2014). Secretion of von Willebrand factor by endothelial cells links sodium to hypercoagulability and thrombosis. Proc. Natl. Acad. Sci. USA *111*, 6485–6490. https://doi.org/10.1073/pnas.1404809111.

27. Nakhaei-Nejad, M., Farhan, M., Mojiri, A., Jabbari, H., Murray, A.G., and Jahroudi, N. (2019). Regulation of von Willebrand Factor Gene in Endothelial Cells That Are Programmed to Pluripotency and Differentiated Back to Endothelial Cells. Stem Cell. *37*, 542–554. https://doi.org/10.1002/stem.2978.

28. Takahashi, K., and Yamanaka, S. (2006). Induction of pluripotent stem cells from mouse embryonic and adult fibroblast cultures by defined factors. Cell *126*, 663–676. https://doi.org/10.1016/j.cell.2006.07.024.

29. Ghaedi, M., and Niklason, L.E. (2019). Human Pluripotent Stem Cells (iPSC) Generation, Culture, and Differentiation to Lung Progenitor Cells. Methods Mol. Biol. *1576*, 55–92. https://doi.org/10.1007/7651_2016_11.

30. González, F., Boué, S., and Izpisúa Belmonte, J.C. (2011). Methods for making induced pluripotent stem cells: reprogramming a la carte. Nat. Rev. Genet. *12*, 231–242. https://doi.org/10.1038/nrg2937.

31. Wang, L., Xiang, M., Liu, Y., Sun, N., Lu, M., Shi, Y., Wang, X., Meng, D., Chen, S., and Qin, J. (2016). Human induced pluripotent stem cells derived endothelial cells mimicking vascular inflammatory response under flow. Biomicrofluidics *10*, 014106. https://doi.org/10.1063/1.4940041.

32. Lian, X., Bao, X., Al-Ahmad, A., Liu, J., Wu, Y., Dong, W., Dunn, K.K., Shusta, E.V., and Palecek, S.P. (2014). Efficient differentiation of human pluripotent stem cells to endothelial progenitors via small-molecule activation of WNT signaling. Stem Cell Rep. *3*, 804–816. https://doi.org/10.1016/j.stemcr.2014.09.005.

33. Bertucci, T., Kakarla, S., Kim, D., and Dai, G. (2022). Differentiating Human Pluripotent Stem Cells to Vascular Endothelial Cells for Regenerative Medicine, Tissue Engineering, and Disease Modeling. Methods Mol. Biol. *2375*, 1–12. https://doi.org/10.1007/978-1-0716-1708-3_1.

34. Grath, A., and Dai, G. (2019). Direct cell reprogramming for tissue engineering and regenerative medicine. J. Biol. Eng. *13*, 14. https://doi.org/10.1186/s13036-019-0144-9.

35. Rufaihah, A.J., Huang, N.F., Kim, J., Herold, J., Volz, K.S., Park, T.S., Lee, J.C., Zambidis, E.T., Reijo-Pera, R., and Cooke, J.P. (2013). Human induced pluripotent stem cell-derived endothelial cells exhibit functional heterogeneity. Am. J. Transl. Res. *5*, 21–35.

36. White, M.P., Rufaihah, A.J., Liu, L., Ghebremariam, Y.T., Ivey, K.N., Cooke, J.P., and Srivastava, D. (2013). Limited gene expression variation

in human embryonic stem cell and induced pluripotent stem cell-derived endothelial cells. Stem Cell. *31*, 92–103. https://doi.org/10.1002/stem.1267.

37. Adams, W.J., Zhang, Y., Cloutier, J., Kuchimanchi, P., Newton, G., Sehrawat, S., Aird, W.C., Mayadas, T.N., Luscinskas, F.W., and García-Cardeña, G. (2013). Functional vascular endothelium derived from human induced pluripotent stem cells. Stem Cell Rep. *1*, 105–113. https://doi.org/10.1016/j.stemcr.2013.06.007.
38. Wang, R., Clark, R., and Bautch, V.L. (1992). Embryonic stem cell-derived cystic embryoid bodies form vascular channels: an in vitro model of blood vessel development. Development *114*, 303–316. https://doi.org/10.1242/dev.114.2.303.
39. Taura, D., Sone, M., Homma, K., Oyamada, N., Takahashi, K., Tamura, N., Yamanaka, S., and Nakao, K. (2009). Induction and isolation of vascular cells from human induced pluripotent stem cells–brief report. Arterioscler. Thromb. Vasc. Biol. *29*, 1100–1103. https://doi.org/10.1161/ATVBAHA.108.182162.
40. Lendahl, U., Muhl, L., and Betsholtz, C. (2022). Identification, discrimination and heterogeneity of fibroblasts. Nat. Commun. *13*, 3409. https://doi.org/10.1038/s41467-022-30633-9.
41. Margariti, A., Winkler, B., Karamariti, E., Zampetaki, A., Tsai, T.N., Baban, D., Ragoussis, J., Huang, Y., Han, J.D.J., Zeng, L., et al. (2012). Direct reprogramming of fibroblasts into endothelial cells capable of angiogenesis and reendothelialization in tissue-engineered vessels. Proc. Natl. Acad. Sci. USA *109*, 13793–13798. https://doi.org/10.1073/pnas.1205526109.
42. Haque, A., Engel, J., Teichmann, S.A., and Lönnberg, T. (2017). A practical guide to single-cell RNA-sequencing for biomedical research and clinical applications. Genome Med. *9*, 75. https://doi.org/10.1186/s13073-017-0467-4.
43. Iacono, G., Massoni-Badosa, R., and Heyn, H. (2019). Single-cell transcriptomics unveils gene regulatory network plasticity. Genome Biol. *20*, 110. https://doi.org/10.1186/s13059-019-1713-4.
44. Francesconi, M., Di Stefano, B., Berenguer, C., de Andrés-Aguayo, L., Plana-Carmona, M., Mendez-Lago, M., Guillaumet-Adkins, A., Rodriguez-Esteban, G., Gut, M., Gut, I.G., et al. (2019). Single cell RNA-seq identifies the origins of heterogeneity in efficient cell transdifferentiation and reprogramming. Elife *8*, e41627. https://doi.org/10.7554/eLife.41627.
45. Wang, K., Lin, R.Z., Hong, X., Ng, A.H., Lee, C.N., Neumeyer, J., Wang, G., Wang, X., Ma, M., Pu, W.T., et al. (2020). Robust differentiation of human pluripotent stem cells into endothelial cells via temporal modulation of ETV2 with modified mRNA. Sci. Adv. *6*, eaba7606. https://doi.org/10.1126/sciadv.aba7606.
46. Chakraborty, S., Ji, H., Kabadi, A.M., Gersbach, C.A., Christoforou, N., and Leong, K.W. (2014). A CRISPR/Cas9-based system for reprogramming cell lineage specification. Stem Cell Rep. *3*, 940–947. https://doi.org/10.1016/j.stemcr.2014.09.013.
47. Krtolica, A., Parrinello, S., Lockett, S., Desprez, P.Y., and Campisi, J. (2001). Senescent fibroblasts promote epithelial cell growth and tumorigenesis: a link between cancer and aging. Proc. Natl. Acad. Sci. USA *98*, 12072–12077. https://doi.org/10.1073/pnas.211053698.
48. The Gene Ontology Consortium, Aleksander, S.A., Balhoff, J., Carbon, S., Cherry, J.M., Drabkin, H.J., Ebert, D., Feuermann, M., Gaudet, P., Harris, N.L., et al. (2023). The Gene Ontology knowledgebase in 2023. Genetics *22*, 1. https://doi.org/10.1093/genetics/iyad031.

STAR★METHODS

KEY RESOURCES TABLE

REAGENT or RESOURCE	SOURCE	IDENTIFIER
Antibodies		
Mouse monoclonal anti-VE-Cadherin (ICC/IHC)	BD Biosciences	Cat#:610251; RRID: AB_397646
Mouse monoclonal anti-CD31 (ICC)	BD Biosciences	Cat#:550389; RRID: AB_2252087
Mouse monoclonal anti-vWF	Fisher Scientific	Cat#:PIMA514029; RRID: AB_11001165
Mouse monoclonal anti-eNOS	Fisher Scientific	Cat#:PIMA515559; RRID: AB_10982295
Mouse monoclonal anti-SOX17	BD Biosciences	Cat#:561590, RRID: AB_10717127
Rabbit monoclonal anti-EphrinB2	Fisher Scientific	Cat#:PIMA532740, RRID: AB_2810017
PE mouse monoclonal anti-VE-Cadherin (FACS)	Fisher Scientific	Cat#:50-106-36; RRID: AB_763438
Alexa Fluor 647 mouse monoclonal anti-CD31 (FACS)	BioLegend	Cat#:303112; RRID: AB_493077
Mouse IgG1, κ	BioLegend	Cat#:400102; RRID: AB_2891079
AlexaFluor594-Ac-LDL	Fisher Scientific	Cat#:L35353
Alexa Fluor 488 goat polyclonal anti-mouse	Fisher Scientific	Cat#:PIA32723; RRID: AB_2633275
Alexa Fluor 647 goat polyclonal anti-mouse	Fisher Scientific	Cat#:PIA32728; RRID: AB_2633277
Alexa Fluor 488 goat polyclonal anti-rabbit	Fisher Scientific	Cat#:PIA32731; RRID: AB_2633280
Bacterial and virus strains		
ETV2 Lentiviral Vector	VectorBuilder	VB170920-1086sma
SOX17 Lentiviral Vector	VectorBuilder	VB240201-1479rbc
Deposited data		
RNA-seq data	This paper	GSE256181
Experimental models: Cell lines		
NHDF-Adult	Lonza	Cat#:CC-2511
NHLF	Lonza	Cat#:CC-2512
HUVEC	Lonza	Cat#:C2519A
Experimental models: Organisms/strains		
7–9-week-old male BALB/c nude mice	Charles River	CAnN.Cg-*Foxn1*^{nu}/Crl
Software and algorithms		
RStudio code for this paper	This paper	https://doi.org/10.5281/zenodo.10659062
iDEP	South Dakota State University	http://bioinformatics.sdstate.edu/idep96/
Geneontology.org	The Gene Ontology Consortium	The Gene Ontology Consortium et al., 2023[48]

RESOURCE AVAILABILITY

Lead contact

Further information and requests for resources and reagents should be directed to and will be fulfilled by the lead contact, Guohao Dai (g.dai@northeastern.edu).

Materials availability

This study did not generate new unique reagents.

Data and code availability

The raw RNA-seq data required to reproduce these findings are available at GEO database (https://www.ncbi.nlm.nih.gov/geo/, accession #: GSE256181). Other data reported in this paper will be shared by the lead contact upon request.

The RStudio code required to reproduce these findings is available at Zenodo. (https://doi.org/10.5281/zenodo.10659062; https://zenodo.org/records/10659062).

Any additional information required to reanalyze the data reported in this paper is available from the lead contact upon request.

EXPERIMENTAL MODEL AND SUBJECT DETAILS

Fibroblast culture and transduction

All biological procedures were performed in sterile conditions in BSL2 biosafety cabinet. All cells were incubated in an incubator at 37°C and 5% CO_2. The NHDF-Ad line used for this project was from a human female and purchased from Lonza (CC-2511). The NHLF line used for this project was from a human male and purchased from Lonza (CC-2512). Fibroblasts were cultured in Fibroblast Growth Medium 2 (FGM-2) (Promocell, C-23020) supplemented with Growth Medium 2 Supplement Mix, 1% penicillin/streptomycin (Gibco, 15140122), and 1% GlutaMax (Gibco, 35050061). Fibroblasts were seeded at 10,000 cells/cm^2, grown overnight, and transduced the next day. The fibroblasts were transduced with an ETV2 lentivirus (ETV2-ECs), a SOX17 lentivirus (SOX17-ECs), or both the ETV2 and SOX17 lentiviruses (rECs) at an MOI of 5 for each virus, in FGM-2 containing 5 μg/mL polybrene (VectorBuilder). These plasmids are Tet-On and will only express ETV2 and SOX17 in the presence of doxycycline. The ETV2 lentiviral vector codes for ETV2 transcript variant 1 (NM_014209.3). The cells were left to incubate with the virus for 48 h, after which the cells were given normal FGM-2. After another 24 h, the cells were given FGM-2 supplemented with 2 μg/mL of puromycin to select for the transduced cells. After 48 h of selection, the cells were again given normal FGM-2 and expanded for future experiments. Fibroblasts were transduced at passage 3 or 4.

Endothelial cell culture

All biological procedures were performed in sterile conditions in BSL2 biosafety cabinet. All cells were incubated in an incubator at 37°C and 5% CO_2. The HUVEC line used for this project was human male/female pooled and purchased from Lonza (C2519A). HUVECs were grown in Endothelial Growth Medium 2 (EGM-2) (Promocell, C-22011) supplemented with Growth Medium 2 Supplement Mix, 1% penicillin/streptomycin (Gibco, 15140122), and 1% GlutaMax (Gibco, 35050061). All ECs were grown on 2% gelatin (Sigma, G1890-100G). For experiments, passages 3–6 were used.

Fibroblast to endothelial cell transdifferentiation

To help drive the reprogramming process, cells were reprogrammed in Endothelial Growth Medium 2 (EGM-2) (Promocell, C-22011) supplemented with Growth Medium 2 Supplement Mix, 1% penicillin/streptomycin (Gibco, 15140122), and 1% GlutaMax (Gibco, 35050061). rECs were given EGM-2 supplemented with 0, 10, 100, 500, 1000, and 2000 ng/mL of doxycycline (Sigma, 50-165-6822). Media was changed every other day. The cells were cultured for 12 days and harvested for RT-qPCR analysis. ETV2 and SOX17 mRNA levels were measured. rECs treated with 1000 ng/mL of doxycycline resulted in high ETV2 and SOX17 expression. Afterward, we cultured rECs in EGM-2 with 1000 ng/mL of doxycycline for 6, 8, 10, 12, and 14 days, after which they were harvested for RT-qPCR analysis. rECs harvested on day 12 were shown to have the highest ETV2 and SOX17 expression. All following experiments reprogram transduced cells with 1000 ng/mL of doxycycline for 12 days unless otherwise stated. For experiments, passages 5–8 were used.

Mice

7∼9-week-old male BALB/c nude mice (CAnN.Cg-*Foxn1*^{nu}/Crl, Charles River) were used for this study. All animal protocols and procedures were reviewed and approved by Northeastern University Animal Care and Use Committee (protocol #19-0210R). Mice were maintained under standard pathogen-free condition and complied with all ethical regulations.

METHOD DETAILS

Quantitative Reverse Transcriptase Polymerase Chain Reaction (RT-qPCR)

RNA was extracted from cells using the RNeasy Mini Kit (QIAGEN, 74106). RNA concentration was quantified using the Nanodrop spectrophotometer (Fisher Scientific, 13-400-518). RT-qPCR analysis was performed using probes from TaqMan Gene Expression Assays and TaqMan Fast Virus 1-Step Master Mix (Applied Biosystems, 44-444-32) on a QuantStudio 3 (Applied Biosystems, A28136) following TaqMan protocols. All mRNA expression measurements were normalized to the expression of RN18S.

Magnetic-activated cell sorting (MACS)

Cells were removed from their culture dish following a typical trypsinization protocol. Cells were spun down using a centrifuge at 300g for 5 min. Cells were reconstituted in 250 μL of PBS. Next, 20 μL of CD31 magnetic beads (Miltenyi Biotech, 130-091-935) were added to the cells and mixed by gentle flicking. The mixture was incubated at 4°C for 20 min, with periodic mixing to ensure that the beads did not settle. After, 5 mL of PBS was added, and the cells were spun at 300g for 5 min. The cells were reconstituted in 1 mL of EGM-2. The magnetic columns were attached to the magnet and primed by putting 1 mL of EGM-2 through them, and then adding the cell suspension. After, the column was removed from the magnet and placed in a 15 mL conical tube. Another 1 mL of EGM-2 was added to the column to allow the $CD31^+$ cells to elute out. The cells were then used in various experiments.

2D immunocytochemistry

Cells were washed with phosphate-buffered saline (PBS) briefly, fixed with 4% paraformaldehyde (Thermo Scientific Chemicals, J19943K2) for 20 min at RT, then washed in PBS 3 times for 5 min each. The cells were then blocked with 10% goat serum (MP Biomedicals, 0219135680) and permeabilized with 0.1% Triton X-(Thermo Scientific Chemicals, A16046AE) simultaneously for 1 h at RT. Cells were then incubated with the primary antibody in 10% goat serum overnight at 4°C. The cells were washed 3 times for 5 min each with PBS. Next, the secondary antibody (1:500) was added and the cells were left to incubate at RT for 30 min. Hoechst 33342 (Thermo Scientific, 62249) was then added directly to the cells without removing the secondary antibody for 15 min at RT. The cells were again washed 3 times for 5 min each and then imaged. Specific antibodies can be found in key resources table.

Brightfield and fluorescent microscopy

An Eclipse Ti2 inverted microscope (Nikon) was used to image cell samples at 4x, 10x, and 20x magnification with Brightfield and various fluorescent filters.

Fluorescent-activated cell sorting (FACS)

Cells were reprogrammed and then lifted from their culture dish using Accutase for 10 min. They were spun down and resuspended in cold FACS buffer (PBS, 10% FBS [Corning, 35011CV], 0.1% sodium azide [Thermo Scientific Chemicals, 447810250], and 0.5 mM EDTA [Fisher Chemical, S311-100]) at a concentration of $1x10^6$ cells/mL. 100 μL of the cell suspension was added to its own tube. Next, the suspension was blocked with 25 μg/mL mouse IgG1 (Biolegend) for 20 min on ice. They were washed 3 times with cold FACS buffer and finally resuspended in 100 μL of cold FACS buffer. The primary antibodies were added to the suspension: 0.25 μL of the Alexa Fluor 647 anti-human CD31 antibody (Biolegend) and 0.5 μL of the PE anti-human VE-CAD antibody (eBioscience). They were incubated at 4°C, in the dark, for 30 min. They were washed 3 times with cold FACS buffer, resuspended in 100 μL of cold FACS buffer, and analyzed immediately using a Beckman Coulter CytoFLEX S Flow Cytometer.

Low-density lipoprotein (LDL) uptake

Reprogrammed cells were incubated with Alexa Fluor 594-Ac-LDL (Fisher Scientific) at a concentration of 10 μg/mL for 4 h. The cells were triple washed with PBS to dispose of excess, unused LDL and then fixed and stained with Hoechst 33342. Next, they were imaged using a fluorescent microscope. LDL uptake was quantified using ImageJ to threshold each image and measure the amount of LDL present in each sample, and then normalizing it to cell count.

Matrigel tubule formation

30 μL of Matrigel (Corning, 354277) was placed in a single well of a 96-well plate. The well plate was placed in the incubator at 37°C for 30 min to allow the Matrigel to solidify. Cells were reprogrammed and sorted into a $CD31^+$ population using MACS. Then, 15,000 cells were seeded on the surface of the Matrigel. The next day, images were taken using Brightfield microscopy.

Inflammatory stimulus response

Cells were reprogrammed and then cultured with 10 ng/mL of tumor necrosis factor alpha (TNF-α) (Invitrogen, A42552) for 6 h. They were washed with PBS 3 times for 5 min each, then harvested for RT-qPCR analysis.

Reprogramming under flow

Cells were reprogrammed and exposed to 48 h of 5 dyn/cm^2 shear stress to evaluate the cells' ability to respond to flow stimuli. Flow was induced using a cone-and-plate shear device (Arcus Technology Inc., DMX-J-SA-17). Briefly, a 1° angled cone spins roughly 100 μm above the confluent cells, causing the cells to experience shear stress according to the following equation:

$$\tau = \frac{\mu\omega}{\theta}$$

where τ is shear stress, μ is the fluid viscosity of EGM-2 at 37°C (0.00078 Pa-s), ω is rotational speed, and θ is the angle of the cone (1°). Media was changed every 24 h and replaced with fresh EGM-2 supplemented with 1000 ng/mL doxycycline. The cells were imaged using Brightfield microscopy and then harvested for RT-qPCR analysis.

RNA-seq data analysis

Cells were reprogrammed and sorted into a $CD31^+$ population using MACS. RNA was isolated using the RNeasy Mini Kit (QIAGEN) and sent to Genewiz for RNA-seq processing. Three programs were used to process the RNA-seq data. RStudio was used to generate heatmaps and principal component analysis plots. iDEP v0.91 from South Dakota State University was used to generate the clusters of the top differentially expressed genes and determine differentially expressed genes between groups. Gene ontology analysis was performed using geneontology.org.

In vivo GelTrex plug assay

Cells were reprogrammed and sorted into a $CD31^+$ population using MACS. We took 700,000 cells and suspended them in 350 μL of GelTrex (Gibco, A1413302), supplemented with 300 ng/mL of bFGF (Gibco, PHG0368) and 10 U/mL of heparin (STEMCELL Technologies, 07980). GelTrex is very similar to Matrigel and was used since it was difficult to acquire Matrigel during the height of the Covid-19 pandemic. There were 5 groups of mice, each treated with a different cell type: Sham (no cells, n = 3), fibroblasts (n = 3), ETV2-ECs (n = 4), rECs (n = 4), or HUVECs (n = 3). The GelTrex suspension was then injected subcutaneously into the abdominal flanks of 7 to 9-week-old male CAnN.Cg-*Foxn1*^{nu}/Crl (BALB/c) mice (Charles River).

After 14 days, the mice were sacrificed, and the plug was excised. The plugs were prepared for cryosectioning by fixing them in 4% PFA for 4 h at RT, then in 30% sucrose (Sigma, S7903-250G) for 18 h at RT. The dehydrated plugs were embedded in O.C.T. compound (Fisher Scientific, 23-730-571), flash frozen using liquid nitrogen, and then stored at −80°C until ready to be sectioned. The frozen plugs were cut into 20 μm slices using a cryostat (Carl Zeiss) and stored on a microscope slide. Brightfield images were taken using a Brightfield microscope.

The slices were then immunostained following a typical cryosection immunohistochemistry protocol to stain for human VE-CAD or human eNOS. First, they were washed in 4% PFA for 10 min. Then, they were washed with PBS twice for 5 min each. They were permeabilized in 0.3% Triton X- for 10 min and then washed again with PBS twice for 5 min each. Next, the samples were placed in 2.95 mg/mL sodium citrate (Fisher Scientific, S279-500) for antigen retrieval and placed in a pressure cooker for 10 min. The samples were then washed with PBS twice for 5 min and had their endogenous peroxidase blocked for 30 min using 1% H_2O_2 (Fisher Scientific, H312-500). They were again washed with PBS twice for 5 min and then blocked with 10% goat serum for 1 h. Primary antibodies were diluted at a 1:50 dilution and placed on the samples overnight. The samples were washed with PBS thrice for 5 min. The secondary antibody was then added at a dilution of 1:500. The samples were mounted with Vectashield (Vector Laboratories, H200010) and imaged immediately.

Blood vessel area was quantified by taking representative Brightfield images of each plug and using ImageJ to calculate the area of red blood cells compared to the area of the plug slice. This process was repeated for each plug and these data points were then averaged together. eNOS expression was quantified by thresholding the fluorescent images and removing the erythrocyte fluorescence, and then measuring the area of eNOS expression compared to the area of the plug slice, again using ImageJ. This was repeated for each sample and averaged together. The total amount of VE-CAD^+ cells in each group was quantified by counting the number of cell nuclei that were in direct contact with the VE-CAD stain. This was then divided by the total cell count to determine what percent of the cells were VE-CAD^+ in each sample. This was repeated for each sample and averaged together.

QUANTIFICATION AND STATISTICAL ANALYSIS

Statistical analyses were performed on all data using a one-way ANOVA or two-sided *t*-tests. HUVEC expression was not part of the one-way ANOVA analysis in Figures 1C, 2G, and 3C. All data presented is presented as mean ± standard deviation (SD) using GraphPad Prism 9. A significance of $p < 0.05$ was used to deem data statistically significant. A $p < 0.01$ is denoted with **, a $p < 0.001$ is denoted with ***, and a $p < 0.0001$ is denoted with ****.